Radiology

Amplitude-modulated Continuous Arterial Spin-labeling 3.0-T Perfusion MR Imaging with a Single Coil: Feasibility Study[1]

Jiongjiong Wang, PhD
Yan Zhang, PhD
Ronald L. Wolf, MD, PhD
Anne C. Roc, MS
David C. Alsop, PhD
John A. Detre, MD

Published online before print
10.1148/radiol.2351031663
Radiology 2005; 235:218–228

Abbreviations:
ASL = arterial spin labeling
CASL = continuous ASL
CBF = cerebral blood flow
ΔM = mean signal change
PASL = pulsed ASL
RF = radiofrequency
ROI = region of interest
SAR = specific absorption rate
SNR = signal-to-noise ratio

[1] From the Departments of Radiology (J.W., Y.Z., R.L.W., J.A.D.) and Neurology (J.W., A.C.R., J.A.D.) and Center for Functional Neuroimaging (J.W., J.A.D.), University of Pennsylvania, 3 W Gates, 3400 Spruce St, Philadelphia, PA, 19104; and Department of Radiology, Beth Israel Deaconess Medical Center, Harvard Medical School, Boston, Mass (D.C.A.). Received October 13, 2003; revision requested January 7, 2004; final revision received May 27; accepted June 17. Supported by National Institutes of Health grants HD39621 and DA015149 and National Science Foundation grant BCS0224007. **Address correspondence to** J.W. (e-mail: *wangj3@mail.med.upenn.edu*).

Authors stated no financial relationship to disclose.

Author contributions:
Guarantors of integrity of entire study, J.W., J.A.D.; study concepts, J.W., J.A.D.; study design, D.C.A., R.L.W., Y.Z., A.C.R.; literature research, J.W., R.L.W.; clinical studies, R.L.W., A.C.R., J.W.; data acquisition, J.W., Y.Z., R.L.W., A.C.R.; data analysis/interpretation, J.W., D.C.A., R.L.W., A.C.R., J.A.D.; statistical analysis, J.W., D.C.A.; manuscript preparation, J.W.; manuscript definition of intellectual content, J.W., D.C.A., J.A.D.; manuscript editing, D.C.A., R.L.W., A.C.R., J.A.D., Y.Z.; manuscript revision/review and final version approval, all authors

Written informed consent was obtained prior to all human studies after the institutional review board approved the protocol. A continuous arterial spin-labeling technique with an amplitude-modulated control was implemented by using a single coil at 3.0 T. Adiabatic inversion efficiency at 3.0 T, comparable to that at 1.5 T, was achieved by reducing the amplitude of radiofrequency pulses and gradient strengths appropriately. The amplitude-modulated control provided a good match for the magnetization transfer effect of labeling pulses, allowing multisection perfusion magnetic resonance imaging of the whole brain. Comparison of multisection continuous and pulsed arterial spin-labeling methods at 3.0 T showed a 33% improvement in signal-to-noise ratio by using the former approach.

Arterial spin-labeling (ASL) perfusion magnetic resonance (MR) imaging has been increasingly adopted for both clinical applications and functional activation studies. Probably the most attractive feature of ASL is that it is noninvasive and repeatable, resulting in a wide variety of applications in neurologic and psychiatric diseases (1–3). The highly reproducible measurements of cerebral blood flow (CBF) with ASL make it suitable for longitudinal studies and repeated examinations for probing of drug effects or vasodilatory reactivity (4–6).

The improved safety of ASL methods is particularly appealing for perfusion imaging in the pediatric population. The normally increased blood flow and water content of a child's brain provides for better image quality (7). ASL perfusion contrast techniques have also enriched the repertoire of tools for functional MR imaging research, complementing methods relying on the blood oxygen level–dependent contrast technique. Potential advantages of perfusion functional MR imaging include improved sensitivity at low task frequencies (8–10), more specific spatial localization (11,12), reduced susceptibility artifact (13), and the ability to provide absolute perfusion quantification (14).

During the past decade, the methodologies for ASL perfusion MR imaging have evolved from feasibility studies into the phase of practical use. However, low signal-to-noise ratio (SNR) remains a weakness of the technique because of both the small fractional effect of the labeled blood (<1% raw signal) and the T1 decay of the labeled arterial blood magnetization during transit from the tagging location to the tissue. Pursuing ASL at high magnetic field strengths (3.0 T and higher) is expected to improve the image quality and reduce transit-related effects on ASL perfusion images by taking advantage of the joint benefits provided by the increased T1 and SNR at high field strengths (15,16). A twofold signal gain is readily achievable by performing pulsed ASL (PASL) at 3.0 and 4.0 T, compared with PASL methods at 1.5 T (15,16), allowing improved spatiotemporal resolution and longer postlabeling delay times to counteract delayed transit effects usually present in the patient population.

The implementation of continuous ASL (CASL) at high magnetic field strengths is expected to provide even greater perfusion contrast and SNR gain than PASL methods at the same field strength (16). Two important challenges of using continuous labeling, however, are controlling for the off-resonance effects caused by radiofrequency (RF) irradiation and achieving ample labeling efficiency within the safety constraints for RF power deposition. Use of a separate small RF coil for labeling can minimize or eliminate the off-resonance effects and may reduce the total RF power by half because generally, no control labeling is required (17,18).

Yet, this dual-coil approach requires special hardware and relies heavily on the labeling geometry, which may vary from subject to subject. The added distance for arterial transit from the carotid tagging region and the relatively poor labeling of the vertebral arteries also limits the practical use of this approach. Alternatively, the off-resonance effects of the labeling pulses can be mimicked by applying control RF irradiation that produces equal off-resonance saturation in the brain tissue (19,20). One such technique employs an amplitude-modulated control based on sinusoid waveforms, equivalent to creating two adjacent inversion planes during the control state so that the net effect on arterial labeling can be neglected (20).

To date, applications of the amplitude-modulated CASL approach have been mainly constrained at 1.5 T. Transplanting this technique to 3.0 T and higher is threatened by reduction in the labeling efficiency when the RF magnitude is decreased to meet the safety limitations on specific absorption rate (SAR) of radiofrequency power at high field strengths. Fortunately, preliminary studies on estimation of CASL efficiency indicated that the efficiency of adiabatic inversion can be maintained over a wide range by keeping the magnitude of the RF pulse and the gradient in proportion (21,22). Thus, the purpose of our study was to test the feasibility of performing amplitude-modulated CASL by using a single coil at 3.0 T.

Materials and Methods

Human Subjects

Thirteen healthy volunteer subjects (five women, aged 24–35 years, with a mean age of 26.8 years ± 5.9 [standard deviation]; and eight men, aged 24–44 years, with a mean age of 33.7 years ± 7.0) underwent MR imaging with a 3.0-T Trio (Siemens, Erlangen, Germany) whole-body imager, by using the product quadrature transmit-receive head coil. There was no statistically significant difference in age between the men and the women.

One additional 41-year-old woman with cerebrovascular disease (bilateral carotid steno-occlusive disease) and one 47-year-old man with a brain tumor (glioblastoma multiforme) were also imaged to test the feasibility of the amplitude-modulated CASL approach in the diagnosis of neurologic disorders. Written informed consent was obtained prior to all human studies after the institutional review board approved the protocol. The volunteers were screened for neurologic and psychiatric disease during consenting processes. In these 13 healthy subjects, five participated in the experiment for optimization of RF and gradient amplitudes, six participated to determine the optimal modulation frequency, six participated to determine the labeling efficiency, one participated to validate the control of off-resonance effect, and nine underwent both CASL and PASL examinations (see the following). No specific criteria were applied for the inclusion of subjects in each experiment, and there were overlaps between the subjects who participated in different experiments.

CASL Imaging Methods

The CASL sequence was based on the prototypical technique developed by Alsop and Detre at 1.5 T (20). The labeling plane was placed 8 cm beneath the center of the imaging sections. Controlling for off-resonance artifacts was effected by applying an amplitude-modulated version of the labeling pulse by using a sinusoidal modulation function. The peak magnitude of the control pulse was $\sqrt{2}$ times the magnitude of the corresponding labeling pulse. The total duration of the labeling and control pulses was 2 seconds, which consisted of 10 repeated RF blocks with a width of 200 msec for each pulse and a 500-μsec gap in between. A gradient-echo echo-planar imaging sequence was used for image acquisition, and a postlabeling delay time of 1 second was inserted between the end of the labeling and control pulses and image acquisition to reduce transit artifact (23).

The choice of the 1-second delay time was based on previous experiments that involved the use of similar imaging parameters at both 1.5 and 4.0 T (16). Acquisition parameters were field of view of 22 cm, 64 × 64 matrix, repetition time msec/echo time msec of 4000/17, bandwidth of 3 kHz per pixel, section thickness of 6 mm, and intersection space of 1.5 mm. Twelve sections were acquired in an inferior to superior direction in a sequential order, and each section acquisition took about 45 msec. Each CASL examination with 80 acquisitions took 5 minutes 20 seconds.

Optimization of CASL Sequence

Earlier work at 1.5 T involved the use of a 2.5-mT/m gradient and 3.5-μT RF irradiation for adiabatic inversion (20). To keep the SAR level at 3.0 T within safety limits (see the following), the magnitude of the labeling pulses was reduced because RF power deposition increases approximately as the square of the field strength (24). Two RF levels (1.50 and 2.25 μT) and three levels of gradient strength (0.8, 1.6, and 2.4 mT/m) were tested to find the optimal parameters that provide the maximum labeling efficiency (with control modulation frequency of 100 Hz). This initial study was performed in the first five of the 13 healthy subjects (two women, three men). A combination of 2.25-μT RF amplitude and 1.6-mT/m gradient was found to provide the best perfusion contrast and was used in subsequent experiments (see Results). The effect of modulation frequency on the CASL perfusion signal was examined in six of the remaining eight healthy subjects (one woman, five men) by using five frequency values (50, 80, 100, 160, and 200 Hz), and an amplitude-modulation frequency of 100 Hz was chosen (see Results).

Off-Resonance Compensation Evaluation

To confirm the ability of the amplitude-modulated control to mimic the off-resonance effects of the labeling, a CASL examination was performed in one healthy volunteer (a 35-year-old woman) with the labeling plane placed distal to (8 cm above the center of) the imaging sections (Fig 1). Since no arterial blood was labeled, the difference images between the labeled and control acquisitions should indicate whether the off-resonance effect was the same in the amplitude-modulated control acquisition as in the labeled acquisition. An RF amplitude of 2.25 μT, a gradient of 1.6 mT/m, and a modulation frequency of 100 Hz were employed for continuous labeling.

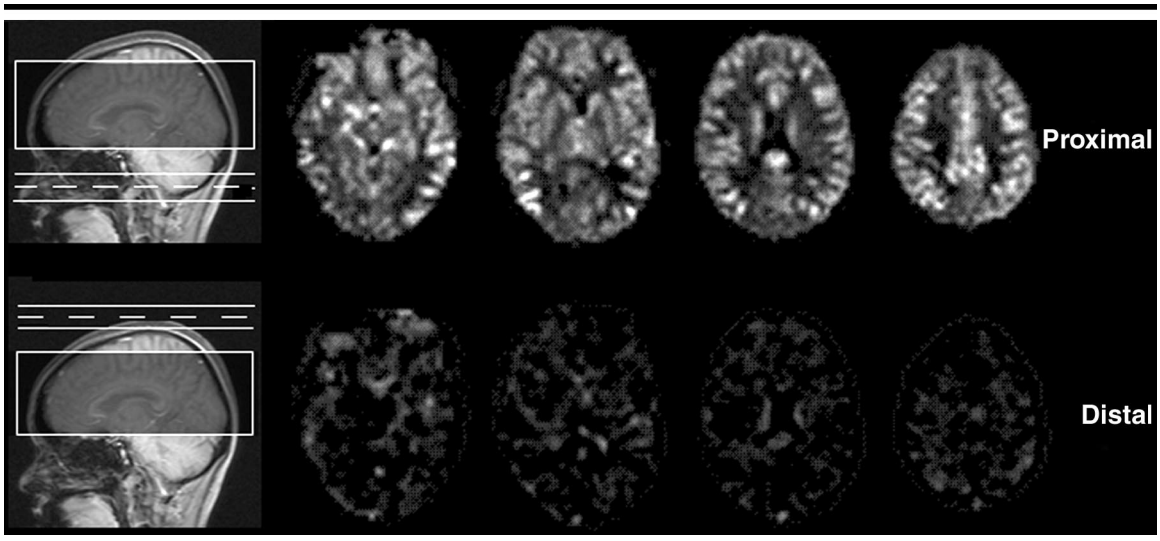

Figure 1. Evaluation of amplitude-modulated control in a healthy subject. Four of 12 transverse sections are shown, acquired by using the 3.0-T CASL method with the labeling plane placed at the pontomedullary junction (proximal) and above the brain (distal). Note that areas of static signal are almost completely subtracted during the distal label state.

Estimation of Labeling Efficiency

The labeling efficiency of the multisection CASL sequence with the amplitude-modulated control was estimated through comparison with the single-section version of CASL technique. In six of the 13 healthy subjects (one woman and five men), perfusion MR images were acquired in a single transverse section through the basal ganglia and thalamus. Images were acquired with both *(a)* the single-section method, in which the label and control were proximal and distal to the imaging section, respectively, and *(b)* the multisection method. In the single-section CASL approach, the sign of the labeling gradient was alternated between the odd and even pairs of proximal and distal labeling acquisitions to reduce imperfections in the subtraction of the labeled and control images (23). All subjects were studied with 1.6-mT/m labeling gradient, 2.25-μT RF irradiation, control modulation frequency of 100 Hz, postlabeling delay of 1 second, and labeling plane offset of 8 cm from the imaging section. On the basis of the ratio between the fractional perfusion signals in these two methods, the labeling efficiency of the multisection CASL method could be estimated.

Comparison with PASL

In nine of the 13 healthy subjects (four women and five men), both CASL (with optimized imaging parameters described earlier) and PASL methods were performed for comparison. The PASL technique was a modified version of the flow-sensitive alternating inversion-recovery technique (25), in which a saturation pulse was applied at TI_1 = 700 msec after global or section-selective inversion (7,16). For optimal labeling, a hyperbolic secant inversion pulse was generated by using MATPULSE software (26) with 15.36-msec duration, 22-μT RF amplitude, and 0.95 tagging efficiency. A gradient of 0.7 mT/m was applied with the hyperbolic secant pulse during tagging, while the hyperbolic secant pulse was applied in the absence of gradient during control acquisition. The slab of the section-selective inversion was 10 cm thick, and the section profile was verified by means of Bloch equation simulation, as well as phantom testing. The saturation pulse was applied to a 10-cm slab adjacent and inferior to the selective inversion slab in both labeled and control acquisitions. A delay time of 1 second was inserted between the saturation and excitation pulses to minimize transit-related effects (23,27). Imaging parameters for the PASL examination were a field of view of 22 cm, 64 × 64 matrix, 3000/17, bandwidth of 3 kHz per pixel, section thickness of 6 mm, and intersection space of 1.5 mm. Twelve sections were acquired in an inferior to superior direction in sequential order with the same coverage as in the CASL examination, and each section acquisition took about 45 msec. Each PASL examination with 80 acquisitions took 4 minutes.

Patient Examination

Two patients with clinical neurologic disorders were included to illustrate the utility and feasibility of the amplitude-modulated CASL technique, one with chronic cerebrovascular disease (left internal carotid artery occlusion and severe steno-occlusive disease of the right internal carotid artery) and the other with a brain neoplasm (glioblastoma multiforme). The imaging parameters were identical to those used for healthy volunteers except for the postlabeling delay time, which was set to 1.2 seconds for the patient with the brain tumor and to 1.5 and 1.8 seconds for the patient with cerebrovascular disease. Two long delay times (with repetition times increased accordingly) were used in the latter case to reduce vascular artifacts due to prolonged transit time. Fluid-attenuation inversion-recovery (9000/84/2500 [inversion time msec]) images and three-dimensional T1-weighted anatomic (1630/3/1100) images were also obtained in these two patients. Structural and CASL perfusion MR images and any relevant prior clinical images were reviewed by a neuroradiologist (R.L.W.).

Data Analysis

For comparison of the SNRs with the PASL and CASL techniques, the raw images acquired by using the two methods were scaled so that the background noise (measured from regions of no signal) was at the same level. A time series of 40 perfusion images of the difference between labeled and control acquisitions was obtained by means of pairwise magnitude subtraction between control and labeled images in each ASL examination, followed by averaging to produce mean

ASL perfusion images (ΔM). SPM99 software (Wellcome Department of Imaging Neuroscience, University College London, England) was used to automatically segment the raw echo-planar images into three regions of interest (ROI) of gray matter, white matter, and cerebrospinal fluid.

The average size of the segmented gray and white matter ROIs was 4562 voxels ± 755 (range, 3501–6069 voxels) and 1544 voxels ± 317 (range, 1295–2370 voxels), respectively. The whole-brain ROI was set as the union of the gray and white matter ROIs (mean, 6106 voxels ± 747; range, 5276–7843 voxels). The mean ΔM signal and raw image intensity were measured within the gray matter, white matter, and whole-brain ROIs to compare the SNR with the PASL and CASL techniques. The two edge sections were excluded from the analyses to avoid possible section profile effects in the PASL examinations.

The SNR efficiency of the PASL and CASL technique, defined as SNR per unit examination time, was further calculated to account for the difference in the repetition time and total examination time of these two methods. The background noise on the raw images acquired by using the two methods (measured from regions of no signal) were divided by the square root of the corresponding examination time ($\sqrt{T_{acq}}$) and then scaled to the same level. The mean ΔM signal and raw image intensity measured within the gray matter, white matter, and whole-brain ROIs after such a scaling process were used to compare the SNR efficiency of the PASL and CASL examinations. Alternatively, SNR efficiency was directly calculated by scaling the measured SNR (see previous explanation) with the square root of the corresponding examination time (SNR efficiency = SNR/$\sqrt{T_{acq}}$), which yielded exactly the same results as those obtained with the former approach.

Because the primary purpose of the present study was to test the feasibility of performing CASL at 3.0 T, T1 maps of brain tissue were not obtained. CBF quantification in the CASL method was approximated by using the following equation, assuming the labeled blood spins remain primarily in the vasculature rather than exchanging completely with tissue water:

$$f = \frac{\lambda \Delta M R_{1a}}{2\alpha M_{con}\{\exp(-wR_{1a}) - \exp[-(\tau + w)R_{1a}]\}}, \quad (1)$$

where α is the tagging efficiency, f is CBF, λ (0.9 mL/g) is the blood-tissue water partition coefficient, M_{con} is the average control image intensity, R_{1a} (0.67 sec^{-1}) is the longitudinal relaxation rate of blood (16), τ (2 sec) is the duration of the labeling pulse, and w (1 sec) is the postlabeling delay time. Equation (1) is deduced from a previous theoretical model (16), which is equivalent to the general kinetic model (28). The calculated CBF values were measured within the gray matter, white matter, and whole-brain ROIs.

SAR Calculation and Monitoring

An estimation of the RF deposition of the 3.0-T CASL sequence was performed by using an analytic solution to a homogeneous sphere as a model for the human head (29). The SAR averaged over the head was given as the following:

$$SAR_{avg} = \frac{\sigma \omega^2 B_1^2 R^2 \tau_{rf}}{10\rho TR}, \quad (2)$$

where B_1 and τ_{rf} are the amplitude and the width of the labeling pulses, respectively; ω is the transmit angular frequency at 3.0 T; R and ρ are the radius and density of the brain, respectively; and σ is the conductivity of the brain. By assuming that $\sigma = 0.6$ siemens per meter, $R = 0.1$ m, and $\rho = 1000$ kg/m^3 (30) and by substituting $B_1 = 2.25$ μT, $\tau_{rf} = 2$ sec, and TR (repetition time) = 4 seconds in Equation (2), the averaged SAR is calculated as 1 W/kg in an adult head of median size.

This estimation does not include the power deposition of the excitation pulses, which will add 10%–20% to the calculated SAR level. The total SAR is below the U.S. Food and Drug Administration guideline of 3 W/kg averaged over the head. The estimated SAR level is consistent with that in a previous study (30), in which the use of numeric simulation yielded 0.75 W/kg for the same labeling pulses (100% duty cycle) used in the present study. The data analysis and SAR calculation were done by one physicist (J.W.) and verified by another physicist (D.C.A.).

In addition to our estimates, the SAR level of a pulse sequence on the 3.0-T MR imager (Trio; Siemens) is calculated automatically by an integrated software program on the basis of the RF pulses, with timing and subject weight used to determine imaging parameters. Reflected power and losses along the transmission line are considered in the vendor calculation. This predicted RF power deposition is expressed as a percentage of the legal requirement value (based on the International Electrotechnical Commission guideline 60601–2-33 for normal operation mode, also approved by the U.S. Food and Drug Administration). If the percentage exceeds 100%, then imaging is not permitted without a change in imaging parameters to reduce the percentage below 100%. During the sequence measurement, the RF power actually deposited is also monitored continuously, and the examination is stopped if this value exceeds the SAR limit-equivalent power threshold. After the examination is finished, an additional consistency check is performed to compare the measured SAR level with the predicted value. If a deviation of more than 10% is observed, an error message is displayed, and the imager has to be rebooted.

Statistical Analysis

The unpaired t test (two-tailed) was employed to compare mean age and SAR level in the two groups of healthy subjects, men and women. The effect of the modulation frequency of the control pulse on the CASL signal was assessed by using the repeated-measures analysis of variance method and the nonparametric Friedman test for related samples in the SPSS 12.0 software package (SPSS, Chicago, Ill). $P < .05$ was considered to indicate a statistically significant difference.

Results

Off-Resonance Compensation

The images of the subtracted difference between labeled and control acquisitions obtained from CASL examinations with distal and proximal labeling are shown in Figure 1. Strong perfusion contrast can be seen when the labeling plane was placed at the pontomedullary junction, while there is barely noticeable residual signal on the images with the label above the brain. Fractional signal change, calculated as the subtracted signal divided by the control image intensity ($\Delta M/M_{con}$), was 0.67% and 0.004% for proximal and distal labeling, respectively.

Optimization of Imaging Parameters

The whole-brain averaged fractional CASL signals ($\Delta M/M_{con}$) acquired with different gradients (0.8, 1.6, and 2.4 mT/m) and RF field amplitudes (1.50 and 2.25 μT) from five healthy subjects are displayed in Figure 2. A set of representative CASL images acquired from one sub-

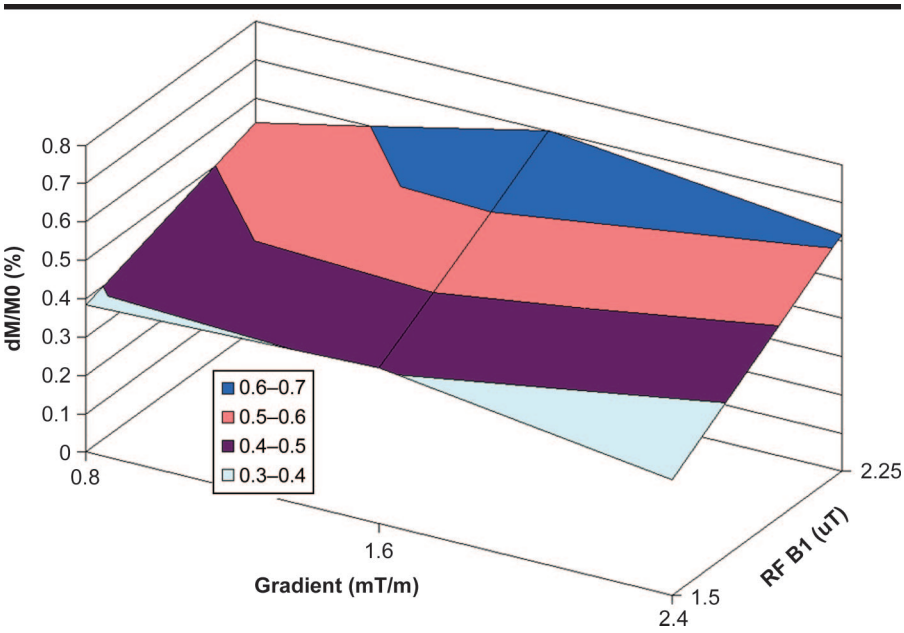

Figure 2. Mean fractional CASL signal (dM/M_{con}) acquired at 3.0 T by using different gradient strengths and RF irradiation. Control modulation frequency is 100 Hz. Peak fractional CASL signal (0.70% ± 0.10) is obtained with 1.6-mT/m gradient and 2.25-μT *(uT)* RF irradiation.

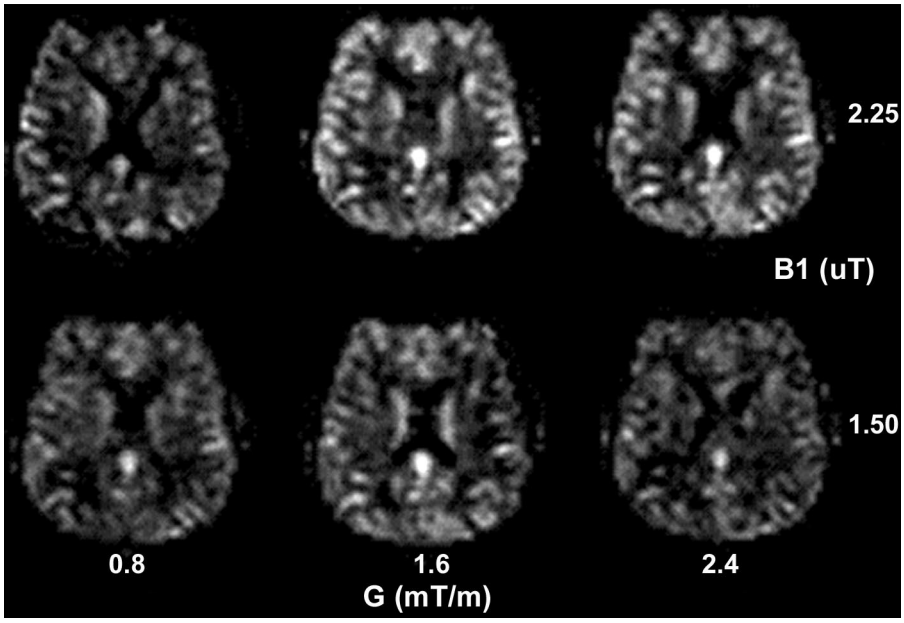

Figure 3. CASL difference perfusion images (Δ*M*) acquired at 3.0 T by using different gradient strengths and RF irradiation in a representative subject. One of 12 transverse sections is shown. Control modulation frequency is 100 Hz. Maximum perfusion contrast is observed with 1.6-mT/m gradient *(G)* and 2.25-μT *(uT)* RF irradiation.

ject is shown in Figure 3. The peak fractional CASL signal (0.70% ± 0.10) is obtained with 1.6-mT/m gradient and 2.25-μT RF irradiation. The optimal ratio between the gradient strength and RF magnitude at 3.0 T is the same as that at 1.5 T (2.5 mT/m and 3.5 μT) (20). The peak fractional CASL signals measured in the gray and white matter ROIs are 0.83% ± 0.13 and 0.41% ± 0.09, respectively, which are in good agreement with reported data acquired by using a dual-coil approach at 3.0 T (17,18).

The fractional CASL signals as a function of the control modulation frequency, acquired by using 1.6-mT/m gradient and 2.25-μT RF in six healthy subjects, are shown in Figure 4. The signals measured in the whole-brain, gray matter, and white matter ROIs are all relatively insensitive to the changes in modulation frequency within the tested range, and the main effect of modulation frequency is not statistically significant by using either the repeated-measures analysis of variance method or the Friedman test for related samples. The frequency of 100 Hz yields the highest mean perfusion signal in the whole-brain and gray matter ROIs. It can also be seen in Figure 4 that the across-subject standard deviation of the measured CASL signals is lowest at the frequency of 100 Hz, suggesting reduced intersubject variability. On the basis of these two observations, the modulation frequency of 100 Hz is used for the CASL method at 3.0 T.

SAR Measurement

Our experiments in the 13 healthy subjects yielded a mean percentage SAR level (measured SAR vs International Electrotechnical Commission guideline 60601–2–33) of 54.5% ± 15.6 (range, 40%–80%) for the CASL method with 2.25-μT RF irradiation. The mean SAR level is significantly higher in men (65.8% ± 12.8) than in women (41.4% ± 0.9) ($P = .005$), probably as a result of the heavier weight in male subjects. During all CASL examinations, the imager was never stopped or rebooted as a result of inconsistency between calculated and measured SAR levels.

Labeling Efficiency Estimation

The CASL images acquired by using the single-section approach and amplitude-modulated control method in a typical subject are displayed in Figure 5. The ratio of the mean CASL signals obtained with the amplitude-modulated and single-section approach is 0.74 ± 0.12 ($n = 6$). If we assume a mean flow velocity of 20 cm/sec (laminar flow with maximum velocity of 40 cm/sec) in the human carotid arteries, the labeling efficiency in the single-section CASL mode has been estimated to be 0.92 with numeric simulation (see Discussion) (22). The labeling efficiency in the amplitude-modulated CASL method at 3.0 T is therefore calculated to be 0.68 (0.92 × 0.74). By using a similar approach, Alsop and Detre (20) have estimated the labeling efficiency to be 0.71 with the amplitude-modulated CASL method at 1.5 T.

Comparison with PASL

The multisection CASL and PASL images acquired in a representative subject are shown in Figure 6. The mean ratio (n = 9) of the SNRs on the CASL versus PASL images is 1.33 ± 0.16 in the whole brain and 1.32 ± 0.22 and 1.49 ± 0.37 in the gray and white matter ROIs, respectively. These values are slightly less than the reported ratio of SNRs in the CASL and PASL methods at 1.5 T (1.47 ± 0.23, whole brain) measured with the same delay time of 1 second (16). When the examination time is taken into account, the mean ratio of the SNR efficiencies with the CASL versus the PASL method is 1.15 ± 0.19 in the whole brain and 1.14 ± 0.19 and 1.29 ± 0.32 in the gray and white matter ROIs, respectively.

By using a previously published theoretical model (16) and incorporating magnetization transfer effects and the T2* difference between blood and brain tissue, the CASL method at 3.0 T is anticipated to produce approximately 2.1 times the PASL signal in the absence of labeling inefficiency (see Appendix). Comparison with our experimental ratio of CASL to PASL suggests a labeling efficiency of approximately 0.6 for the multisection CASL method. This value is reasonably compatible with the labeling efficiency of 0.68 estimated earlier by other means. However, the estimation from comparison with PASL may be less straightforward than the former approach, as the theoretical model depends on assumptions of multiple parameters, such as T1 and T2*, exchange time, and size of the magnetization transfer effect. The PASL signal may also be susceptible to potential errors caused by labeled venous blood and section profile effects of the inversion and saturation pulses. Therefore, we use 0.68 as the best estimate of the labeling efficiency for the present technique.

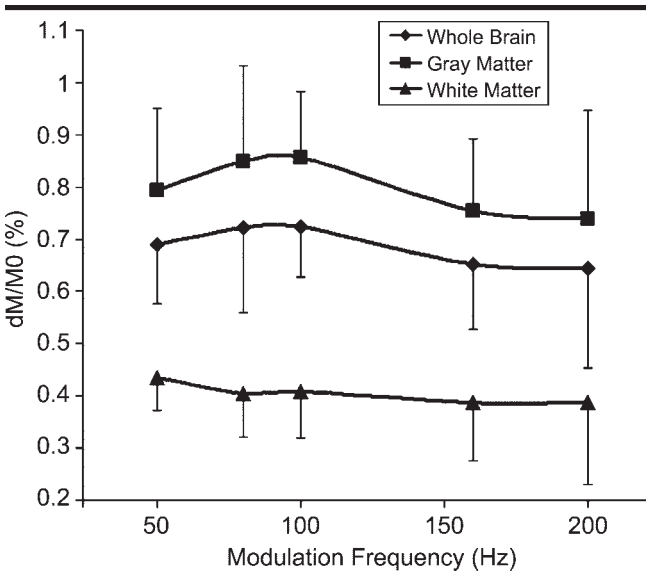

Figure 4. Mean fractional 3.0-T CASL signal ($\Delta M/M_{con}$) as a function of control modulation frequency measured in whole-brain, gray matter, and white matter ROIs. Error bars indicate the standard deviation across subjects. Data were acquired with 1.6-mT/m gradient and 2.25-μT RF irradiation. Main effect of modulation frequency is not statistically significant.

Figure 5. Comparison of the difference perfusion images acquired with single-section *(SS)* CASL method and amplitude-modulated *(AM)* CASL technique in a representative subject. Single transverse section is shown. Ratio of mean CASL signals obtained with amplitude-modulated and single-section approach is 0.74 ± 0.12.

CBF Quantification with CASL

The calculated mean CBF (n = 11) based on Equation (1) and 0.68 labeling efficiency is 40.2 mL/100 g/min ± 4.3 in the whole brain and 49.5 mL/100 g/min ± 6.2 and 22.4 mL/100 g/min ± 4.0 in the gray and white matter ROIs, respectively. The small variance of the CBF measurements in this cohort of healthy subjects lends support for the technique's stability across subjects. Equation (1) assumes that the labeled blood stays in the vasculature rather than completely exchanging into the tissue compartment, which may lead to underestimation of perfusion, since brain T1 is shorter than blood T1, especially in the presence of off-resonance effects. On the other hand, we use the control image intensity (M_{con}) to represent the equilibrium magnetization of brain (M_0) in Equation (1), which may result in overestimation of perfusion by ignoring the brain signal loss due to T2* relaxation at the echo time. As suggested by our theoretical model (Appendix), the overall effect is about 7% underestimation in perfusion quantification.

Patient Data

For clinical examples, the difference perfusion images (ΔM) were evaluated rather than the quantitative CBF images to avoid potential quantification error in calculating CBF due to uncertain parameters in pathologic states. The two sets of difference perfusion images acquired with delay times of 1.5 and 1.8 seconds in the patient with cerebrovascular disease are displayed in Figure 7. Delayed transit effects (intravascular hyperintensities) are present on difference perfusion images acquired with the 1.5-sec delay time and are more evident in the right hemisphere than in the left. With a longer delay (1.8 sec), transit artifacts are greatly reduced, while

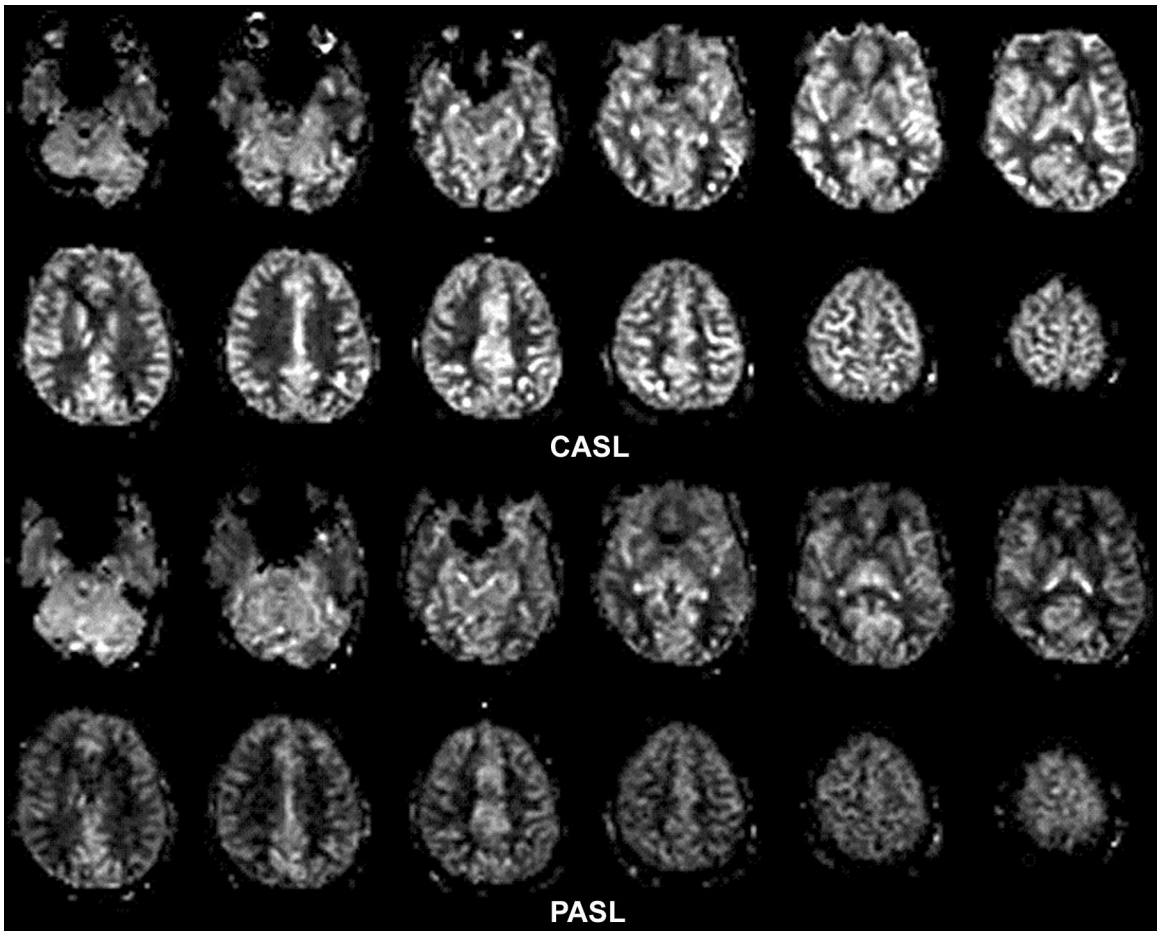

Figure 6. Comparison of 12 transverse sections of difference perfusion images (ΔM) acquired by using amplitude-modulated CASL technique and PASL method in a representative subject at 3.0 T. Background noise on CASL and PASL perfusion images is scaled at the same level. Mean ratio of SNRs and SNR efficiencies in CASL versus PASL method is 1.33 and 1.15 in the whole brain, respectively.

image quality is preserved. Such long delay times (>1.5 seconds) were not feasible at 1.5 T (1–3). The T2-weighted fluid-attenuation inversion-recovery and CASL perfusion images acquired in the patient with glioblastoma multiforme are shown in Figure 8. The whole-brain coverage of the CASL method allows a full evaluation of the status of blood flow in this extensive brain tumor, and heterogeneous flow conditions are observed in the tumor regions. This illustrates the potential ability of the CASL method in guiding biopsy and depicting regions of increased CBF that are associated with neovascularity (and thus higher tumor grade) (31).

Discussion

The present study demonstrated the feasibility of performing amplitude-modulated CASL with a single coil at 3.0 T. The measured CBF values in healthy adults are in agreement with results reported by other investigators who used ASL techniques (23,27,32,33). The power deposition caused by the long labeling RF pulses is within the SAR limit. It is possible that the SAR level with the current imaging parameters might approach or even exceed 100% in subjects with extremely heavy weight or large head size. In this case, the problem can be solved easily by increasing the repetition time appropriately.

Our data also confirm the previous observation that an amplitude-modulated control pulse provides an excellent match of the off-resonance effect in the adiabatic labeling pulses (20), allowing multisection perfusion images that cover the whole brain. When compared with CASL methods that involve the use of a separate coil for labeling, the single-coil amplitude-modulated technique is easier to implement in clinical MR systems without the need for special hardware. It is also more convenient for patient handling and provides more uniform labeling of both anterior and posterior circulation. While the overall SAR level averaged over the head or body may be lower in the dual-coil methods, the local power deposition around the tagging site is complicated and needs to be assessed meticulously, given the spatially constrained RF irradiation (34).

Our experimental results indicate that continuous labeling efficiency at 3.0 T is comparable with that at 1.5 T, despite a roughly one-third reduction in the magnitude of the RF pulses, which is consistent with a previous finding (22) that the inversion efficiency can be preserved by simultaneously reducing the amplitudes of the gradient and RF pulses. A more recent theoretical work (21) suggested that the optimal RF amplitude for adiabatic inversion is linearly proportional to

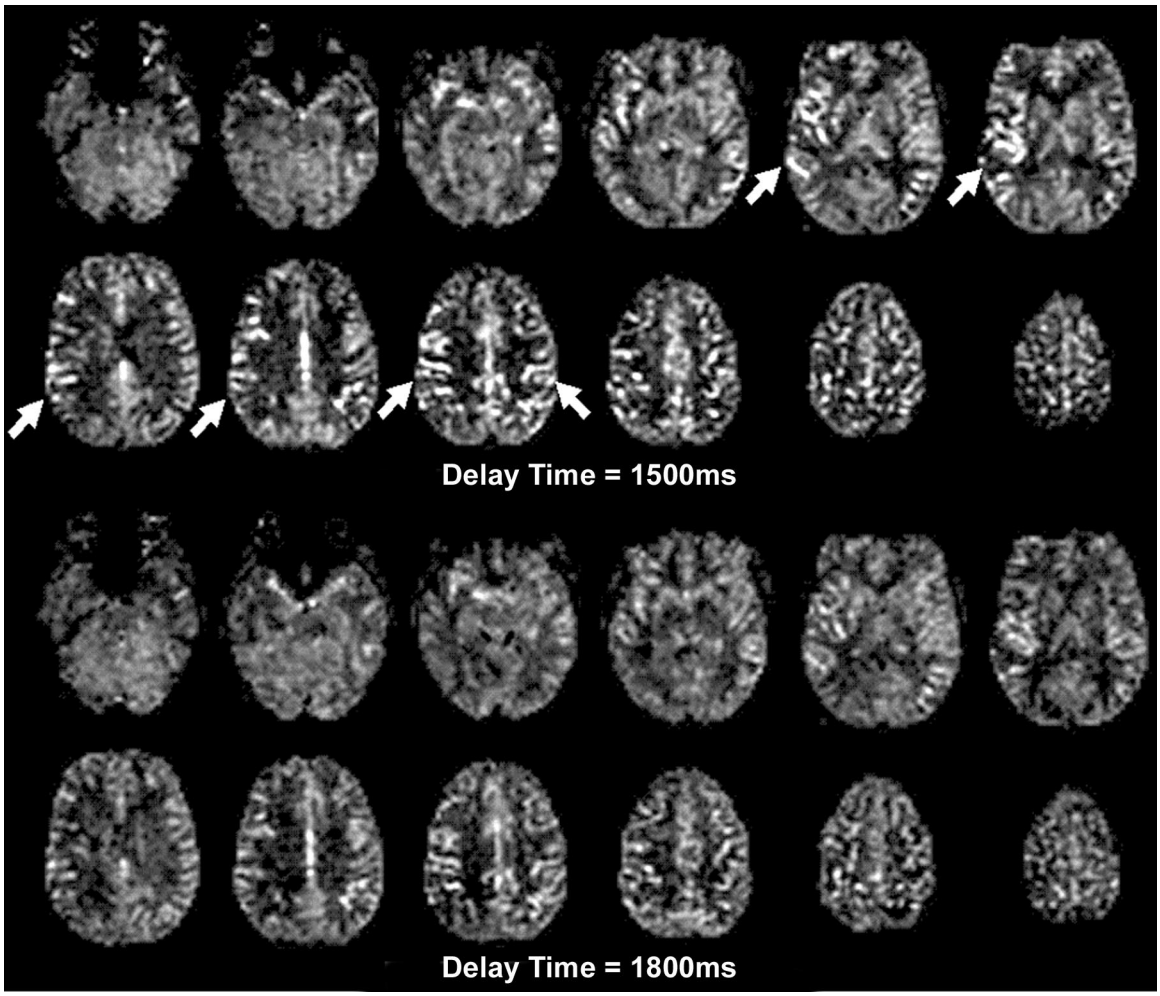

Figure 7. Perfusion-weighted images (Δ*M*) acquired by using amplitude-modulated CASL method at 3.0 T with postlabeling delay times of 1.5 and 1.8 seconds in a 41-year-old woman with bilateral carotid steno-occlusive disease. Twelve transverse sections are shown. Vascular artifacts (arrows) are greatly reduced at longer delay time without apparent deterioration of perfusion image quality.

the square root of the gradient amplitude. Although the general trend of the changes in the gradient and RF amplitude seems to agree with that model, our experimental data do not suggest a square root increase of RF with gradient strength. Our data show relative insensitivity of the CASL signal to the control modulation frequency, in contrast to previous results (20) that showed an increase in labeling efficiency with reduced modulation frequency.

The basis of this discrepancy remains uncertain. The previous observation (20) was made at 1.5 T with 2.5-mT/m gradient and 3.5-μT RF irradiation, and the authors claimed that their results did not agree with theoretical calculation. It is possible that the effect of modulation frequency will be distinct at different settings of gradient and RF amplitude. The search for optimal parameters may need to be performed in three-dimensional parameter space of gradient, RF, and modulation frequency. Because we were limited by time and on the basis of implications from previous studies, we performed a two-dimensional search for optimal combination of gradient and RF and then determined the optimal modulation frequency at that chosen setting of gradient and RF amplitude. Further experimental and theoretical work may be needed to understand the interactions between these parameters and to find the potential best point in three-dimensional space for maximization of labeling efficiency.

The estimated labeling efficiency of 0.68 in the amplitude-modulated CASL method relies on the accuracy of the assumed efficiency of 0.92 in the single-section CASL method. Although this labeling efficiency was estimated by means of numeric simulation with T1 and T2 values at 1.5 T, the value is expected to be similar at 3.0 T. This is because T2 relaxation dominates the inefficiency of adiabatic inversion, and T2 of arterial blood changes little from 1.5 to 3.0 T, assuming 100% oxygen saturation in the arterial blood (35). In the dual-coil approach, the labeling efficiency is generally estimated to be close to 100% at the tagging site (17,18). Because of the methodologic similarity between the single-section CASL and adiabatic inversion with a separate coil, a labeling efficiency of more than 0.9 is reasonable in the single-section CASL method.

In a recent study (36), investigators measured the continuous labeling efficiency in a saline flow phantom by using the single-section approach. The results showed an efficiency of 0.85 for a mean flow velocity of 26.4 cm/sec with 2.5-

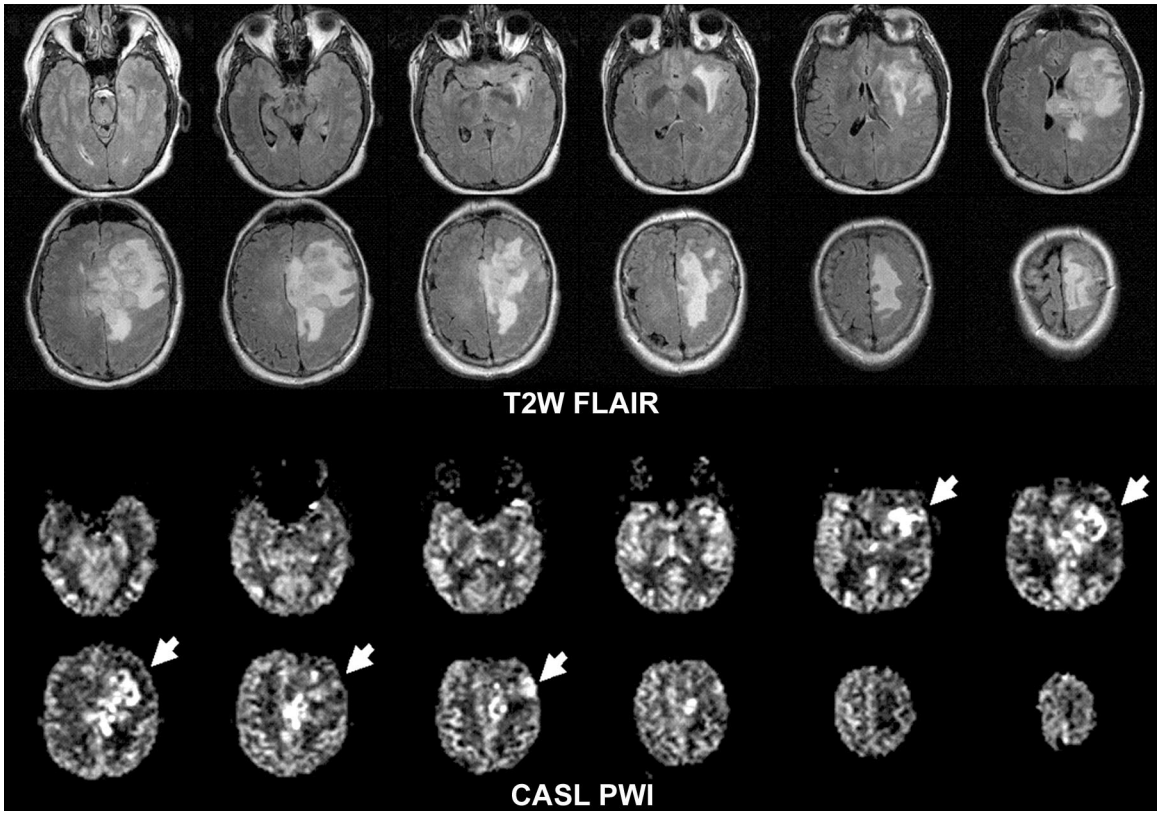

Figure 8. T2-weighted fluid-attenuation inversion-recovery images *(T2W FLAIR)* and perfusion-weighted images *(PWI)* acquired by using the amplitude-modulated CASL method at 3.0 T in a 47-year-old man with glioblastoma multiforme. Twelve transverse sections are shown. Perfusion images show heterogeneous blood flow (arrows) in tumor regions.

mT/m gradient and 2.25-μT RF irradiation. With an approximate 7% increase in efficiency by using a gradient of 1.6 instead of 2.5 mT/m, the predicted efficiency with the imaging parameters used in our experiments will be 0.91, which is a very close match with our assumption. The current CASL technique involved the use of a high labeling duty cycle (>99%) and is thus relatively immune to the errors caused by discontinuous labeling pulses (21,36). The fluctuations of flow velocity within a cardiac cycle tend to have minimum effect on the estimation of inversion efficiency, since the mean flow velocity provides a fairly acceptable simplification for adiabatic inversion, as suggested in other studies (21,36).

One interesting observation from the current study is that the SNR gain in the CASL method as opposed to PASL seems to be reduced at 3.0 T when compared with 1.5 T. Besides the small difference in the labeling efficiencies at these two field strengths, increased susceptibility effect at high magnetic field strengths may affect the measured signal change. Two recent studies (16,37) suggested that the short T2* of brain tissue at high field strengths may affect the accuracy of resting perfusion measurement, as well as the effect size of signal change induced by task activation in ASL techniques. Specifically, because more labeled blood spins exchange into brain tissue in CASL than in PASL (in general), the CASL method pays a heavier toll of signal loss due to fast T2* relaxation in the brain tissue. This T2* effect becomes more severe at high field strengths, which may lead to reduced SNR gain seen in the CASL methods. Spin-echo–based image acquisition schemes (such as spin echo echo-planar or fast spin echo) or fast gradient-echo methods with ultrashort echo times (such as SPIRAL or partial k-space echo-planar) should result in a greater labeling effect than the employed gradient-echo echo-planar acquisitions.

Another possibility is that the high-duty cycle of the RF amplifier during the labeling period may add thermal noise to the CASL data, thus degrading the SNR gain as opposed to PASL methods, which use almost instantaneous labeling pulses. This argument seems unlikely on the basis of our phantom test results, which showed no difference in the background noise of the CASL and PASL images. We used a postlabeling delay time of 1 second in the CASL examination. A small amount of vascular (hyperintense intraluminal) signals can be observed in the resultant perfusion images of some subjects, attributed to a high concentration of labeled spins in arteries that have not exchanged with the microvasculature or tissue. Nevertheless, the reported results should not be affected by the precise location of the label at the time the image is acquired, since they are measured over large ROIs and represent the total labeling effect in both the vasculature and the brain tissue.

Several limitations exist in the present study, which need further exploration. The first issue concerns the consistency of the labeling efficiency in the presence of variable flow velocities in patients and increased B_1 inhomogeneity at high field strengths. This concern of reduced labeling efficiency is based on the theoretical calculation that reduced RF irradiation allows a narrower range of flow velocities for optimal adiabatic inversion (22). To achieve a labeling efficiency of more than 0.9, a B_1 of 3.5 μT at 1.5 T allows a mean

$$\frac{\Delta M}{M_{con}} = \frac{-2f\alpha}{\lambda \exp(-TER_{2*tissue})} \left\{ \begin{array}{l} \left[\exp(-wR_{1a}) - \exp((\min(\delta - w, 0) - \delta)R_{1a})\right]\exp(-TER_{2*blood})/R_{1a} + \\ \exp(-\delta R_{1a})\left\{ \begin{array}{l} \dfrac{\exp(-wR_{1ns})}{R_{1s}}\left[1 - \exp(\min(\delta - \tau, 0)R_{1s})\right] + \\ \dfrac{1}{R_{1ns}}\left[\exp(\min(\delta - w, 0)R_{1ns}) - \exp(-wR_{1ns})\right] \end{array} \right\}\exp(-TER_{2*tissue}) \end{array} \right\}$$

Figure A1. Equation for CASL ΔM signal. α Is labeling efficiency; f is CBF; δ is tissue transit time (1.4 sec) (40); λ is the blood-tissue water partition coefficient (0.9 mL/g); M_{con} is raw control image intensity; R_{1a} is longitudinal relaxation rate of arterial blood (0.67 sec^{-1}); R_{1s} (1.15 sec^{-1}) and R_{1ns} (0.81 sec^{-1}) are longitudinal relaxation rates of brain tissue with and without off-resonance RF saturation, respectively; $R_{2*tissue}$ (28.6 sec^{-1}) and $R_{2*blood}$ (5.0 sec^{-1}) are transverse relaxation rates of brain tissue and arterial blood, respectively; τ is duration of labeling pulses (2 sec); and w is postlabeling delay time (1.0–1.5 sec due to sequential image acquisition).

$$\frac{\Delta M}{M_{con}} = \frac{-2M_0 f\alpha}{\lambda \exp(-TER_{2*tissue})} \left\{ \begin{array}{l} \exp(-TIR_{1a})\left[w - (\min(\delta - w, 0) - \delta)\right]\exp(-TER_{2*blood}) + \\ \exp(-TIR_{1ns})\left[\exp(\min(TI, \delta + TI_1)\Delta R) - \exp(\delta \Delta R)\right]\exp(-TER_{2*tissue})/\Delta R \end{array} \right\}$$

Figure A2. Equation for PASL ΔM signal, where α is 0.95 in PASL, $\Delta R = R_{1ns} - R_{1a}$, TI is image acquisition time (1.7–2.2 sec), and TI_1 is duration of tagging bolus (0.7 sec).

velocity range of about 10–40 cm/sec, while a B_1 of 2.25 μT at 3.0 T allows about 5–25 cm/sec mean velocity range.

Similarly, the tolerance of B_1 inhomogeneity is lower at 3.0 T than at 1.5 T. According to both our experimental data and other studies (22,36), an RF amplitude of around 2.0 μT seems to be the lower limit for achieving adequate inversion efficiency for human flow velocity range. The accuracy and efficiency of the current CASL technique may deteriorate if the degree of B_1 inhomogeneity exceeds 12%. Another issue that needs to be addressed is the T1 effect on the accuracy of CBF quantification. We did not include the T1 maps of brain tissue in the calculation of CBF images in the present study. Ignoring the difference between T1s of blood and brain tissue could result in potential errors in CBF measurements—for example, an underestimation of flow in short-T1 tissues, such as white matter, and an overestimation of flow in long-T1 tissues, such as an edematous lesion in the gray matter (3).

Although our theoretical calculation demonstrates about 7% underestimation of perfusion in healthy adult subjects, the accuracy of perfusion measurements by using the simplified model (Eq [1]) in pathologic conditions cannot be predicted. To bring the 3.0-T CASL method into real clinical use, further study will be needed to refine the perfusion model by taking into account the specific pathophysiologic conditions of each brain disorder.

The current amplitude-modulated CASL technique may not be directly applied at 4.0 T or higher field strength because the RF amplitude has to be reduced to be lower than 1.7 μT without increasing the repetition time. At this level of RF irradiation, the labeling efficiency will be less than 0.5. A new development in performing flow-driven adiabatic inversion at high field strengths is to simultaneously modulate the RF and gradient by the same amplitude waveform while adjusting the frequency of the RF irradiation to preserve the inversion plane location (38).

By reversing the signs of the RF and gradient halfway through the labeling period between label and control, the magnetization transfer effects can be well controlled. The immediate benefit of using the simultaneous modulation of the RF and gradient for labeling is that the tagging efficiency is improved by using labeling pulses with very low irradiation. Although this approach is more demanding in terms of hardware performance compared with the amplitude-modulated method, its feasibility at both 1.5 and 3.0 T has been demonstrated. Another alternative approach is to perform pseudocontinuous inversion with a train of saturation pulses (39). The SAR level is expected to be low enough for perfusion imaging at 4.0 T or even higher, while the labeling efficiency can still be kept close to 0.5.

In conclusion, an amplitude-modulated CASL method has been implemented successfully at 3.0 T with a single transmit-receive coil. The improved image quality and potential convenience for patient management should bring ASL techniques into the realm of practical clinical use.

Appendix

The present theoretical calculation is based on the two-compartment perfusion model (16) in which the observed ΔM signal consists of signals from tissue and arterial vascular compartments. An important effect missing from the CASL model in reference 16 was the transverse signal relaxation, which is considered to be relatively small at 1.5 T, since the T2*s of brain and blood are much longer than the echo time. At 3.0 T and higher field strengths, this effect may affect the accuracy of perfusion measurement, since echo time is comparable with the T2* of brain tissue. By incorporating transverse relaxation in equations (A2) and (A3) in reference 16, the CASL ΔM signal is given by the equation in Figure A1 in the present study. The presumption of the equation in Figure A1 is $\tau + w > \delta$, which is always satisfied in our experiments.

Similarly, the PASL ΔM signal is given by the equation in Figure A2.

The presumption of the equation in Figure A2 is $TI > \delta$, which is always satisfied in our experiments. By substituting the assumed parameters into the equations in Figures A1 and A2 and by including the measured ratio of 1.33 between the CASL and PASL signal, the labeling efficiency with the CASL method is 0.6. At a given CBF level (eg, 60 mL/100 g/min), the equation in Figure A1 yields a fractional signal change of 0.69%, while Equation (1) yields 0.74%. This will result in 7% underestimation of perfusion by using the simplified model (Eq [1]).

Acknowledgment: The authors are grateful to Michael Szimtenings, PhD, from Siemens Medical Solutions for providing information on the product SAR calculation.

References

1. Detre JA, Alsop DC, Vives LR, Maccotta L, Teener JW, Raps EC. Noninvasive MRI evaluation of cerebral blood flow in cerebrovascular disease. Neurology 1998; 50: 633–641.
2. Alsop DC, Detre JA, Grossman M. Assessment of cerebral blood flow in Alzheimer's disease by spin-labeled magnetic resonance imaging. Ann Neurol 2000; 47: 93–100.
3. Chalela JA, Alsop DC, Gonzalez-Atavalez JB, Maldjian JA, Kasner SE, Detre JA. Magnetic resonance perfusion imaging in acute ischemic stroke using continuous arterial spin labeling. Stroke 2000; 31:680–687.
4. Yen YF, Field AS, Martin EM, et al. Test-retest reproducibility of quantitative CBF measurements using FAIR perfusion MRI and acetazolamide challenge. Magn Reson Med 2002; 47:921–928.
5. Detre JA, Samuels OB, Alsop DC, Gonzalez-At JB, Kasner SE, Raps EC. Noninvasive MRI evaluation of CBF with acetazolamide challenge in patients with cerebrovascular stenosis. J Magn Reson Imaging 1999; 10: 870–875.
6. Floyd TF, Ratcliffe SJ, Wang J, Resch B, Detre JA. Precision of the CASL-perfusion MRI technique: global and regional cerebral blood flow within vascular territories at one hour and 1 week. J Magn Reson Imaging 2003; 18:649–655.
7. Wang J, Licht DJ, Jahng GH, et al. Pediatric perfusion imaging using pulsed arterial spin labeling. J Magn Reson Imaging 2003; 18:404–413.
8. Wang J, Aguirre GK, Kimberg DY, Detre JA. Empirical analyses of null-hypothesis perfusion fMRI data at 1.5 and 4 T. Neuroimage 2003; 19:1449–1462.
9. Aguirre GK, Detre JA, Zarahn E, Alsop DC. Experimental design and the relative sensitivity of BOLD and perfusion fMRI. Neuroimage 2002; 15:488–500.
10. Wang J, Aguirre GK, Kimberg DY, Roc AC, Li L, Detre JA. Arterial spin labeling perfusion fMRI with very low task frequency. Magn Reson Med 2003; 49:796–802.
11. Duong TQ, Kim DK, Ugurbil K, Kim SG. Localized cerebral blood flow response at submillimeter columnar resolution. Proc Natl Acad Sci U S A 2001; 98:10904–10909.
12. Luh WM, Wong EC, Bandettini PA, Ward BD, Hyde JS. Comparison of simultaneously measured perfusion and BOLD signal increases during brain activation with T(1)-based tissue identification. Magn Reson Med 2000; 44:137–143.
13. Wang J, Li L, Roc AC, et al. Reduced susceptibility effect in perfusion fMRI using single-shot spin-echo EPI acquisitions. Magn Reson Imaging 2004; 22:1–7.
14. Detre JA, Wang J. Technical aspects and utilities of fMRI using BOLD and ASL. Clin Neurophysiol 2002; 113:621–634.
15. Yongbi MN, Fera F, Yang Y, Frank JA, Duyn JH. Pulsed arterial spin labeling: comparison of multi section baseline and functional MR imaging perfusion signal at 1.5 and 3.0 T: initial results in six subjects. Radiology 2002; 222:569–575.
16. Wang J, Alsop DC, Li L, et al. Comparison of quantitative perfusion imaging using arterial spin labeling at 1.5 and 4.0 Tesla. Magn Reson Med 2002; 48:242–254.
17. Zaharchuk G, Ledden PJ, Kwong KK, Reese TG, Rosen BR, Wald LL. Multislice perfusion and perfusion territory imaging in humans with separate label and image coils. Magn Reson Med 1999; 41:1093–1098.
18. Mildner T, Trampel R, Moller HE, Schafer A, Wiggins CJ, Norris DG. Functional perfusion imaging using continuous arterial spin labeling with separate labeling and imaging coils at 3 T. Magn Reson Med 2003; 49:791–795.
19. Talagala SL, Noll DC. Functional MRI using steady state arterial water labeling. Magn Reson Med 1998; 39:179–183.
20. Alsop DC, Detre JA. Multi section cerebral blood flow MR imaging with continuous arterial spin labeling. Radiology 1998; 208:410–416.
21. Utting JF, Thomas DL, Gadian DG, Ordidge RJ. Velocity-driven adiabatic fast passage for arterial spin labeling: results from a computer model. Magn Reson Med 2003; 49:398–401.
22. Maccotta L, Detre JA, Alsop DC. The efficiency of adiabatic inversion for perfusion imaging by arterial spin labeling. NMR Biomed 1997; 10:216–221.
23. Alsop DC, Detre JA. Reduced transit-time sensitivity in noninvasive magnetic resonance imaging of human cerebral blood flow. J Cereb Blood Flow Metab 1996; 16:1236–1249.
24. Schaefer DJ. Safety aspects of magnetic resonance imaging. In: Wehrli FW, Shaw D, Kneeland JB, eds. Biomedical magnetic resonance imaging. New York, NY: YCH, 1988; 553–574.
25. Kim SG. Quantification of relative cerebral blood flow change by flow-sensitive alternating inversion recovery (FAIR) technique: application to functional mapping. Magn Reson Med 1995; 34:293–301.
26. Matson GB. An integrated program for amplitude-modulated RF pulse generation and re-mapping with shaped gradients. Magn Reson Imaging 1994; 12:1205–1225.
27. Wong EC, Buxton RB, Frank LR. Quantitative imaging of perfusion using a single subtraction (QUIPSS and QUIPSS II). Magn Reson Med 1998; 39:702–708.
28. Buxton RB, Frank LR, Wong EC, Siewert B, Warach S, Edelman RR. A general kinetic model for quantitative perfusion imaging with arterial spin labeling. Magn Reson Med 1998; 40:383–396.
29. Haacke EM, Brown RW, Thompson MR, Venkatesan R. Magnetic resonance imaging. New York, NY: Wiley, 1999.
30. Collins CM, Smith MB. Signal-to-noise ratio and absorbed power as functions of main magnetic field strength, and definition of "90" RF pulse for the head in the birdcage coil. Magn Reson Med 2001; 45: 684–691.
31. Warmuth C, Gunther M, Zimmer C. Quantification of blood flow in brain tumors: comparison of arterial spin labeling anddynamicsusceptibility-weightedcontrast-enhanced MR imaging. Radiology 2003; 228: 523–532.
32. Ye FQ, Mattay VS, Jezzard P, Frank JA, Weinberger DR, McLaughlin AC. Correction for vascular artifacts in cerebral blood flow values measured by using arterial spin tagging techniques. Magn Reson Med 1997; 37:226–235.
33. Yang Y, Frank JA, Hou L, Ye FQ, McLaughlin AC, Duyn JH. Multislice imaging of quantitative cerebral perfusion with pulsed arterial spin labeling. Magn Reson Med 1998; 39:825–832.
34. Strilka RJ, Li S, Martin JT, Collins CM, Smith MB. A numerical study of radiofrequency deposition in a spherical phantom using surface coils. Magn Reson Imaging 1998; 16:787–798.
35. Wright GA, Hu BS, Macovski A. Estimating oxygen saturation of blood in vivo with MR imaging at 1.5 T. J Magn Reson Imaging 1991; 1:275–283.
36. Gach HM, Kam AW, Reid ED, Talagala SL. Quantitative analysis of adiabatic fast passage for steady laminar and turbulent flows. Magn Reson Med 2002; 47:709–719.
37. Lawrence KS. Effects of the apparent transverse relaxation time on cerebral blood flow measurements obtained using arterial spin tagging: a theoretical investigation (abstr). In: Proceedings of the Eleventh Meeting of the International Society for Magnetic Resonance in Medicine. Berkeley, Calif: International Society for Magnetic Resonance in Medicine, 2003; 668.
38. Alsop DC. Improved efficiency for multislice continuous arterial spin labeling using time varying gradients (abstr). In: Proceedings of the Ninth Meeting of the International Society for Magnetic Resonance in Medicine. Berkeley, Calif: International Society for Magnetic Resonance in Medicine, 2001; 1562.
39. Detre JA, Leigh JS, Williams DS, Koretsky AP. Perfusion imaging. Magn Reson Med 1992; 23:37–45.
40. Wang J, Alsop DC, Song HK, et al. Arterial transit time imaging with flow encoding arterial spin tagging (FEAST). Magn Reson Med 2003; 50:599–607.